Final Draft

of the original manuscript

Ben Khalifa, N.; Thiery, S.:

Incremental sheet forming with active medium.

In: CIRP Annals. Vol. 68 (2019) 1, 313 - 316.
First published online by Elsevier: 24.04.2019

https://dx.doi.org/10.1016/j.cirp.2019.04.043

Incremental sheet forming with active medium

Noomane Ben Khalifa [a,b], Sebastian Thiery [a]

[a] Institute of Product and Process Innovation, Leuphana University of Lüneburg, Volgershall 1, 21339 Lüneburg, Germany
[b] Helmholtz Zentrum Geesthacht, Institute of Materials Research, Max Planck Str 1, D-21052 Geesthacht, Germany

Sponsored by Matthias Kleiner (1), TU Dortmund, Germany

A new process combining incremental sheet forming and the use of an active medium to produce concave-convex geometrical parts is introduced. Both, experiments and finite element modeling, pursue the objective of explaining the basic forming mechanism and of discussing the influence of the active medium pressure on the overall process feasibility. Results show that the active medium, in this case gas, acts as an active supplementary tool under controlled pressure, thus enabling the manufacture of concave-convex parts which could not be easily produced by conventional incremental sheet forming.

1. Introduction

Single point incremental forming (SPIF) is, due to its low investment costs, a suitable process for small-batch production and rapid prototyping [1]. In contrast to conventional sheet metal forming processes, SPIF does not require a die, but instead a tool progressively generating the geometry of a part by following a predefined path [2]. This process has been widely addressed in the literature, and various improvements of this process have been developed to reduce process time, to increase material formability and accuracy and to extend the product range.

The product range of SPIF is restricted to concave shapes. One way to manufacture convex features is to rotate the blank during the process, with the tool working alternately on one side of the blank. This process is called back-drawing incremental forming (BIF) [3]. The rotation of the blank can be done manually by unclamping, turning and repetitive clamping or automatically if the clamping system has a rotational axis [3]. Another way to manufacture concave-convex shapes is two-point incremental forming (TPIF), which defines the final geometry by the support of a die [4]. Because each die is used for only one specific shape, TPIF is less flexible as SPIF [5]. Duplex incremental forming (DPIF) uses a second tool on the opposite side of the blank. Both tools change the role as forming or supporting tool and can create complex free- form surfaces in one clamping [6], but the synchronisation of tool paths remains challenging [7].

To reduce process time, TPIF can be combined with stretch forming (SF) to create a pre-form and to superimpose tensile stresses during the deformation by the tool [8]. An additional benefit of combining these processes is a more uniform thickness distribution [8]. An active medium can also be used to create a pre- form in a two-stage forming strategy [9]. At the first stage, an aluminium blank of 1 mm thickness was formed into a hemispherical shell using hydraulic oil at a pressure of 5 MPa. A truncated cone was manufactured by SPIF at the second stage. The advantages of this two-stage strategy include the improved maximum forming depth and sheet thinning [9]. Another possibility to reduce the process time is the use of multiple forming tools working simultaneously on the same side of the blank [10].

SPIF has also been improved by adding a medium used to heat the blank, Fig. 1a. For example, Galdos et al. [11] used oil to deform magnesium blanks at 250 °C, showing that the formability could thereby be increased. Mohammadi et al [12] reduced the local springback of aluminium parts by also heating the blanks up to 260 °C with hot air.

Different media have been also used as a soft support and for pressure superposition during SPIF. Conducting a numerical investigation of an aluminium blank and a pressure of 0.02 MPa, Kumar and Kumar [13] showed that superposition by pressure increases the formability of the material and reduces the force on the tool. Mcloughlin et al. [14] used compressed air at 0.035 MPa to softly support the bottom surface of an aluminium blank. Their results showed, that support by the medium did not result in greater accuracy. They observed bulging up to 5 mm at the base of the part. This effect was, however, not used to deliberately create a convex shape.

The aim of this paper is to provide a new approach to geometrically controlling this bulging effect, which could be used to manufacture convex part. This new process is called incremental forming with active medium (IFAM). The active medium applies a controlled pressure to the bottom surface of the blank. The tool creates the concave features of a part by conventional SPIF, but the pressure can also invert the forming direction and act as a supplementary tool to shape convex features. Concave-convex parts are manufactured in one clamping without a die or a second tool, which was not possible in previous studies.

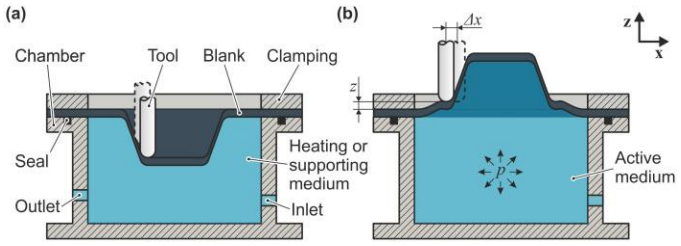

Figure 1. (a) Heating medium or soft support during concave forming, (b) incremental forming with active medium (IFAM) for convex shapes.

This paper provides a general process description of IFAM and describes the experimental setup. A numerical model shows the stress and strain distribution and identifies the area of plastic deformation. In a next step, an analytical model for the relationship between the wall angle α and the pressure p is developed. Results from experiments with different combinations of process parameters are discussed and compared to the analytical model. Finally, the process feasibility is verified by showing concave- convex sample parts manufactured by IFAM.

2. Process description and setup

Fig. 1b depicts the principle of IFAM. The blank is fixed by a blank holder to a pressure chamber to create a closed system. Sealing has to be included between the blank and the back plate of the pressure chamber to avoid leakages. The chamber contains the active medium, which could be compressed air, hydraulic oil or water. An inlet for the active medium is needed, but an outlet would only be required if a constant flow of the active medium were necessary. The pressure chamber is mounted to the bench of a CNC milling machine, and the machine spindle moves the forming tool. IFAM works with similar hemispherical tools used in SPIF.

After pressure is applied to the blank, the tool incrementally shapes the part. The tool follows a predefined path in both concave and convex forming processes. In the case of concave forming, the tool moves from the margins towards the centre of the blank along the contour of the desired shape. The final shape, then, is mainly influenced by the tool path. In contrast, the tool moves from the centre towards the margins in convex forming processes. The tool moves primarily parallel to the **xy** plane and therefore does not follow the individual form of the desired shape, Fig. 2b. The pressure only elastically deforms the blank. In combination with the tool, however, the material plastically flows in a positive **z** direction at the contact zone of the tool and the blank. With every cycle, the positive deformation incrementally increases, and the final convex shape gradually emerges. Besides the vertical position of the tool z, the incremental step size in the horizontal plane Δx

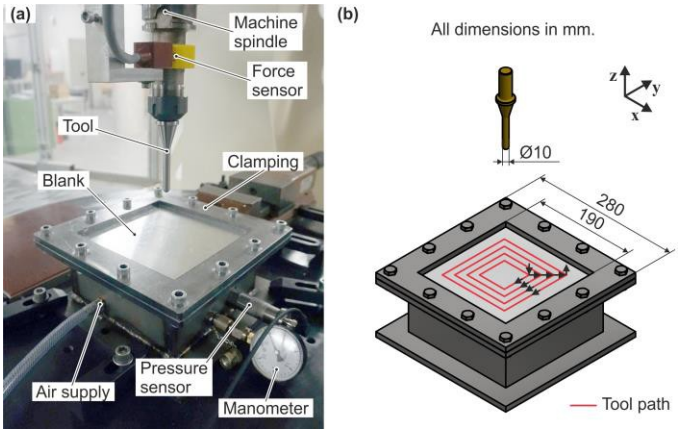

Figure 2. (a) Experimental setup for IFAM, (b) dimensions and tool path.

and the pressure p affect the outcome of the process. These main parameters have to be appropriately adapted to the position and radius of the tool, the blank's dimensions and material and, most importantly, the desired shape. Feed rate and rotational speed of the tool may also play a role.

The experimental setup, Fig. 2a, for IFAM is placed on a 5-axis high- speed milling portal centre. The blank material is aluminium AA1050A-H14 with a thickness of 1 mm; the dimensions inside the clamping are 190 mm x 190 mm. A forming oil is applied to the blank to reduce wear. A tool with a diameter of 10 mm is used, and the tool holder includes an axial force sensor. The active medium is compressed air, and pressure is measured relative to atmosphere. A LabVIEW programme records the pressure and the force on a measurement computer. To observe the tool position, a connection between the computer and the CNC is established. A control valve can adjust the pressure during the process to create the desired shape. The following numerical and analytical investigations relate to this experimental setup.

3. Numerical and analytical modeling

3.1. Strain and stress distribution

To understand how IFAM creates the shape of the part, a numerical model using Abaqus with an explicit solver is developed to show the strain and stress distribution. The element type is solid element (C3D8R). Mass scaling is deactivated when the pressure is applied to or removed from the blank, and it is used moderately during tool movement. To reduce calculation time, the feed rate is artificially increased to 60,000 mm/min.

The blank has the same dimensions as in the setup and is divided into four layers of elements over the thickness. Concerning length and width, the element size is set to 1 mm for the entire blank, resulting 144,400 elements in total. Elastic-plastic material behaviour is assumed with a combined hardening law and with von Mises yield criterion. Plasticity is defined by Ludwik with an initial flow stress of 90 MPa. The tool with a diameter of 10 mm is a rigid body, and the influences of friction or rotational speed are neglected. At the beginning of the simulated process, the pressure increases linearly to 0.06 MPa, and the tool subsequently moves to its vertical position z = 0 mm. The tool trajectory is a unidirectional square and includes seven cycles with a horizontal step size Δx = 1 mm. The square of the first cycle has a width of 120 mm and of the final cycle a width of 132 mm. The simulated process needs 3.7 s, the real process 213 s. The calculation time is 246 hours with the programme running on two cores.

Fig. 3 reveals that there is no plastic deformation solely through the pressure p. Just the material at the contact zone with the tool starts to flow

plastically; the rest of the blank remains elastic. The area of plastic deformation incrementally increases with every cycle of the tool. The wall angle α seems to be influenced by the pressure p but also by the number of cycles. At least several cycles are needed until a specific wall angle α emerges. Because the plastic deformation only occurs in response to the tool due to stress concentration, the blank becomes thinner only in this

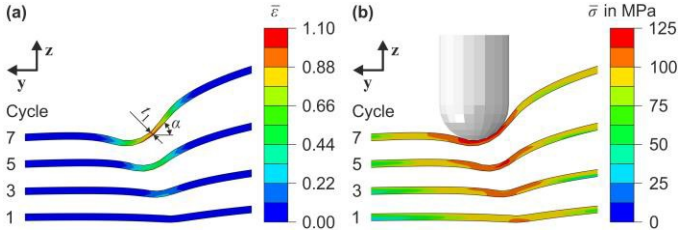

Figure 3. (a) Equivalent plastic true strain $\bar{\varepsilon}$ and (b) equivalent stress $\bar{\sigma}$ in the cross section through **yz** plane for different cycles.

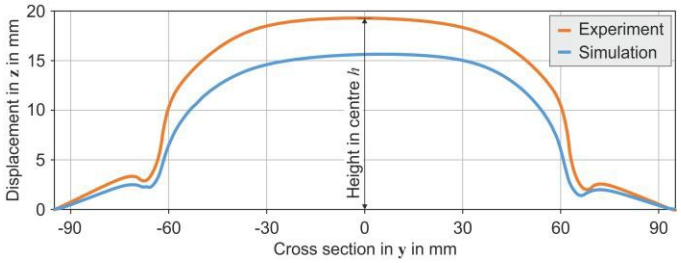

Figure 4. Comparison of the final displacement in **z** direction for the cross section through **yz** plane between the simulation and the experiment.

region. Thinning increases with the angle, and it can be assumed that the wall thickness t_1 can be expressed by the sine law as in SPIF, as described in Ref. [3], depending on the wall angle α.

To validate the numerical model, the final height in cross section (Fig. 4) is compared between the simulation and an experiment using the same process parameters. The simulation shows a similar convex deformation as the experiment, although the effect is weaker with a smaller height h in the centre of the blank.

3.2. Relation between wall angle and pressure

The relationship between convex forming and the pressure of the active medium can be described as a force equilibrium between the stress in the contact zone and the vertical force caused by the pressure. Grzancic et al. [15] developed an equation to predict the forming force on an indenting tool by multiplying the membrane force σ_M with the loaded area A_{load} (Fig. 5). Because the tool is not fully surrounded by blank material in IFAM, the equation is modified by adding a proportional factor ξ_A to calculate the resulting force F_r, Eq. 1. The proportional factor ξ_A is 0.5 during the first cycle, but smaller in all subsequent ones.

$$F_r = \xi_A \cdot 2 \cdot \pi \cdot R \cdot t_1 \cdot \sigma_f \cdot sin^2\alpha \tag{1}$$

The total vertical force created by the medium is the product of pressure p and the blank area, which is calculated using the dimension a inside the clamping. Because this force is distributed to both the tool and the clamping, the resulting force F_r accounts for a smaller share and is expressed by the proportional factor ξ_p, Eq. 2. It can be assumed that only half of the area inside one tool cycle with the dimension b is involved in the force equilibrium at the tip of the tool. The factor ξ_p is then calculated as ratio between the area enclosed by the tool path and the blank area, Eq. 3.

$$F_r = \xi_p \cdot a^2 \cdot p \tag{2}$$

$$\xi_p = \frac{b^2}{2 \cdot a^2} \tag{3}$$

Assuming that the thinning of the blank in IFAM is similar to the one in SPIF, Eq. 4, and that plane strain condition are present [1], the true strain in thickness direction ε_t, Eq. 5, can be used to calculate the equivalent strain $\bar{\varepsilon}$, Eq. 6. The flow stress $\sigma_f(\bar{\varepsilon})$ is then a function of the strain.

$$t_1 = t_0 \sin(90° - \alpha) = t_0 \cdot \cos\alpha \tag{4}$$

$$\varepsilon_t = \ln(\cos\alpha) \tag{5}$$

$$\bar{\varepsilon} = \frac{2}{\sqrt{3}} \cdot |\varepsilon_t| = \frac{2}{\sqrt{3}} \cdot |\ln(\cos\alpha)| \tag{6}$$

Combining these six equations, one can express the pressure $p(\alpha)$ in terms of the wall angle α, Eq. 7, with $0° \leq \alpha < 90°$. The function $p(\alpha)$ has a global maximum p_{max}. This value has to be

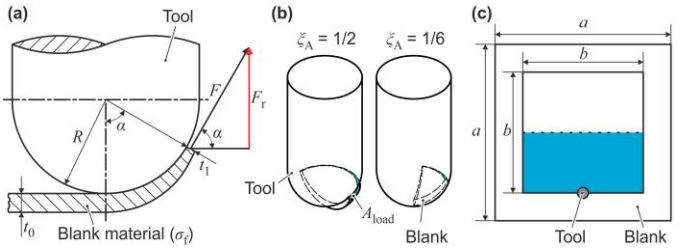

Figure 5. (a) Force at tool contact modified from Grzancic et al. [15], (b) loaded area at tool contact and (c) involved area of the blank.

exceeded if one is to produce high angle; under these circumstances, cracks might, however, appear due to instability.

$$p(\alpha) = \frac{\xi_A \cdot 2 \cdot \pi \cdot R \cdot t_0 \cdot \sigma_f(\bar{\varepsilon}) \cdot sin^2\alpha \cdot \cos\alpha}{\xi_p \cdot a^2} \tag{7}$$

4. Experimental verification

4.1. Influence of pressure

Simulations are not suitable to verify the analytical model because the computational time would be too long. For this reason, experiments for different pressure levels were conducted to identify the minimal required pressure to initialise the process of convex forming. The final geometry is represented by the height of the part h measured at the centre after the process. Table 1 defines the four different tool paths used for the experiments.

Convex shapes emerge slowly at low pressures, but as pressures increases, they grow rapidly until the material cracks, Fig. 6. The higher the number of cycles n, the easier it is to determine the minimum required pressure. For example, the tool moved always on the same rectangle (Δx = 0 mm; n = 38) multiple times, and cracks already occurred at 0.035 MPa. Having a last cycle of same dimensions, the tool path with a greater number of cycles (Δx = 0.25 mm; n = 25) showed a higher sensitivity towards the pressure p, whereas the tool path with fewer cycles (Δx = 1 mm; n = 7) was more stable. Compared to the latter, the sensitivity was only slightly higher if the step size was smaller but the number of cycles the same (Δx = 0.25 mm; n = 7).

The global maximum p_{max} of the function $p(\alpha)$, Eq. 7, is calculated for the previous experiments. ξ_A=1/6 and b = 120 mm are assumed, and the flow curve of the material is described by Ludwik, Eq. 8.

Table 1
Tool path definition for experiments; rotational speed is 300 1/min and vertical tool position z = 0 mm for all experiments.

Δx in mm	n	Dimensions of first cycle in mm	Dimensions of last cycle in mm	Feed rate in mm/min
0.00	38	120 x 120	120 x 120	2,000
0.25	7	120 x 120	123 x 123	1,000
0.25	25	120 x 120	132 x 132	1,000
1.00	7	120 x 120	132 x 132	1,000

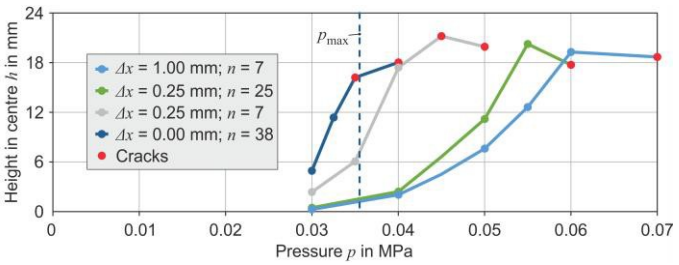

Figure 6 Influence of the pressure p on the final part height h at different horizontal step sizes Δx and different number of cycles n.

$$\sigma_f(\bar{\varepsilon}) = 90.542 + 38.458 \cdot \bar{\varepsilon}^{0.132} \quad (8)$$

As result, the angle $\alpha = 55.654°$ requires the maximal pressure $p_{max} = 0.036$ MPa. This value has to correlate with the smallest pressure causing cracks in experiments, Fig. 6. The obtained value $p = 0.035$ MPa verifies that the analytic model is approximately correct for a horizontal step size $\Delta x = 0$ mm. The analytical model is not applicable for a horizontal step size $\Delta x > 0$ mm, but p_{max} can be regarded as the minimal required pressure for convex forming.

4.2. Feasibility

The analytical model and the experiments show that the shape of the parts can be controlled by adjusting the pressure p. Because convex and concave features can be combined in any way desired, it is possible to create a wide range of geometrical shapes. To evaluate process feasibility, a sample part with an outer cone and an inner pyramid was manufactured using IFAM, Fig. 7b and Fig. 7c. There are two processes for producing this part, concave- convex or convex-concave, both beginning at the centre. The tool paths and the pressure p were defined manually, Table 2. Both bigger outer shapes and smaller inner shapes can be created by IFAM, and different geometries can be combined.

A reference part manufactured by BIF, Fig. 7a, was the target shape for both IFAM processes. Part (b) shows an uncontrolled bulging in the transition region due to the pressure, and the position of the inner feature deviates from the target shape. Nevertheless, IFAM increased accuracy in the clamping area. Part (c) is characterized by low shape accuracy of the inner feature because it was not possible to create a sharp edge at the bottom of the pyramid. It is, however, the most accurate part in the transition region. In short, IFAM partially increased accuracy compared to BIF, but it could not achieve the good overall accuracy of DPIF, e.g. reported by Ndip-Agbar et al. [16]. Algorithms for generating tool paths and pressure levels are currently not available but could increase the accuracy of IFAM in the future. Because IFAM is feasible with milling machines and does not need customized setups, it has the potential for industrial application.

Table 2
Process parameters for manufacturing convex features.

Part	Region	p in MPa	Δx in mm	z in mm
(b)	Outer cone	0.070-0.045	1.00	0.0
(c)	Inner pyramid	0.075-0.070	0.50	3.0-1.5

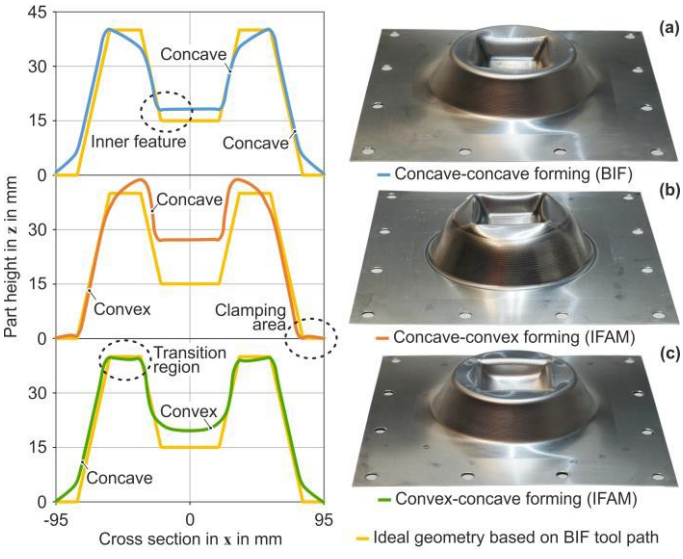

Figure 7. Sample part manufactured by BIF (a), outer convex forming (b), inner convex forming (c) and cross sections compared to ideal geometry.

5. Conclusion

A new process involving pressure by an active medium during single point incremental forming was introduced. Convex forming is primarily influenced by the pressure and increases with pressure level. This mechanism could be analytically explained as force equilibrium in the contact region between tool and blank. Process feasibility was established by manufacturing sample parts with changing curvatures and by combining different geometries. Future studies need to apply the analytical model for other material properties and for other blank and tool dimensions. Investigations should also focus on strategies for improving geometrical accuracy. To deepen one's understanding of this new process, residual stresses or process limits such as the maximum wall angle need to be further investigated.

Acknowledgments

The authors would like to thank the German Research Foundation (DFG) for the support of this research project under the grant number BE 5196/14-1. The assistance by Prof. Paulo A. F. Martins provided for this project is greatly appreciated. The authors also want to express their gratitude towards the Institute of Forming Technology and Lightweight Components (IUL) for its support.

References

[1] Martins PAF, Bay N, Skjoedt M, Silva MB (2008) Theory of Single Point Incremental Forming. *CIRP Annals–Manufacturing Technology* 57(1):247–252.

[2] Jeswiet J, Micari F, Hirt G, Bramley A, Duflou J, Allwood J (2005) Asymmetric Single Point Incremental Forming of Sheet Metal. *CIRP Annals–Manufacturing Technology* 54(2):88–144.

[3] Ambrogio G, De Napoli L, Filice L, Micari F, Muzzupappa M (2006) Some Considerations on the Precision of Incrementally Formed Double-curvature Sheet Components. *Proceedings of the 9th ESAFORM Conference on Material Forming,* 199-202.

[4] Formisano A, Durante M, Langella A, Capece Minutolo F (2008) A Comparison Between Two Incremental Forming Processes for the Achievement of a Component with Concave-convex Shape. *Proc. 4th Virtual Conference on Innovative Production Machines and Systems*, 498-503.

[5] Silva MB, Martins PAF (2013) Two-Point Incremental Forming with Partial Die: Theory and Experimentation. *Journal of Materials Engineering and Performance* 22(4): 1018-1027.

[6] Meier H, Magnus C, Smukala V (2011) Impact of Superimposed Pressure on Dieless Incremental Sheet Metal Forming With Two Moving Tools. *CIRP Annals–Manufacturing Technology* 60(1):327–330.

[7] Bambach M (2008) *Process Strategies and Modelling Approaches for Asymmetric Incremental Sheet Forming*, *Umformtechnische Schriften, Band* 139. Shaker Verlag, Aachen.

[8] Taleb Araghi B, Maco GL, Bambach M, Hirt G (2009) Investigation Into a New Hybrid Forming Process: Incremental Sheet Forming Combined with Stretch Forming. *CIRP Annals–Manufacturing Technology* 58(1):225–228.

[9] Shamsari M, Mirnia MJ, Elyasi M, Baseri H (2018) Formability Improvement in Single Point Incremental Forming of Truncated Cone Using a Two-stage Hybrid Deformation Strategy. *International Journal of Advanced Manufacturing Technology* 94(5-8):2357-2368.

[10] Wernicke S, Dang T, Gies S, Tekkaya AE (2018) Effect of Multiple Forming Tools on Geometrical and Mechanical Properties in Incremental Sheet Forming. *AIP Conference Proceedings* 1960(1):160031.

[11] Galdos L, Sáenz de Argandoña E, Ulacia I, Arruebarrena G (2012) Warm Incremental Forming of Magnesium Alloys Using Hot Fluid as Heating Media. *Key Engineering Materials* 504-506:815-820.

[12] Mohammadi A, Vanhove H, Weise D, Van Bael A, Landgrebe D, Duflou JR (2017) Influence of Global Forced-air Warming on the Bulge Formation in Shallow Sloped SPIF parts. *Procedia Engineering* 183:149-154.

[13] Kumar Y, Kumar S (2018) Analysis of Pressure Assisted Incremental Sheet Forming Process Through Simulation. *International Journal of Mechanical and Production Engineering Research and Development* 8(3):921-932.

[14] Mcloughlin K, Cognot A, Quigley E (2003) Dieless Manufacturing of Sheet Metal Components with non Rigid Support. *Proc. SheMet 2003*, 123-130.

[15] Grzancic G, Löbbe C, Ben Khalifa N, Tekkaya AE (2019) Analytical Prediction of Wall Thickness Reduction and Forming Forces During the Radial Indentation Process in Incremental Profile Forming. *Journal of Material Processing Technology* 267:68-79.

[16] Ndip-Agbor E, Ehmann K, Cao J (2018) Automated Flexible Forming Strategy for Geometries With Multiple Features in Double-Sided Incremental Forming. *Journal of Manufacturing Science and Engineering* 140(3): 031004.